



Can Groundwater Scenarios Be Predicted from Future Regional Climatic Input Variables?

Satiprasad Sahoo¹ · Anirban Dhar² · Anupam Debsarkar³ · Amlanjyoti Kar⁴

Received: 13 November 2018 / Accepted: 8 October 2020 /

Published online: 13 October 2020

© Springer Nature B.V. 2020

Abstract

Conjunctive use of water is an integral part of water resources management. Future groundwater scenarios will dictate the water management policies. The present research focuses on future groundwater scenario generation based on regional scale CMIP5 data. The future scenarios for the years 2030, 2050 and 2080 were generated in terms of the groundwater potential zones (GWPZs) with seven futuristic parameters [land use and land cover, maximum temperature, minimum temperature, rainfall, groundwater recharge, groundwater table and evapotranspiration (ET)]. The Dyna-CLUE and MIROC5 were used for generation of the future change in climate and land use/land cover scenarios. The Soil and Water Assessment Tool (SWAT) was utilized for the recharge and ET estimation. Future groundwater heads were calculated by using the Modular Three-Dimensional Finite-Difference Groundwater Flow (MODFLOW). Bias corrected rainfall and temperature data of Representative Concentration Pathways (RCP 4.5) were utilized. Total twelve water quality parameters (pH, Cl^- , Mg^{2+} , F^- , Na^+ , EC, TH, HCO_3^- , K^+ , Ca^{2+} , SO_4^{2-} and PO_4^{2-}) were used for groundwater quality zone (GWQZ) mapping. These GWPZ and GWQZ were divided into three (poor potential, moderate potential, and good potential) and four zones (good quality, moderate quality, poor quality and above permissible limit) respectively. The lower part of the basin was identified as poor GWPZ (35.76% for 2030) and GWQZ due to an increase in urban areas. However, the middle and upstream portion covers good, moderate zones. Field-based soil moisture and groundwater level monitoring data were utilized for validation purposes. It was observed that groundwater level < 5 m bgl corresponds to good GWPZ. It was also observed that recharge and pH were the crucial parameters for good GWPZ (+11.83%) and GWQZ (-21.31%) according to sensitivity analysis.

Keywords AHP · Dyna-CLUE · GIS · Groundwater potential · Groundwater quality · MIROC5 · MODFLOW · SWAT

✉ Satiprasad Sahoo
satisps@gmail.com

1 Introduction

Anthropogenic activities heavily influence groundwater potential and quality (Dhanasekarapandian et al. 2016). Groundwater continuously moves from recharge to discharge areas depending on the local hydraulic gradient. Rainfall and anthropogenic discharges (e.g., wastewater) act as the main sources of recharge. Moreover, groundwater scenarios depend on the dynamic changes in land use/land cover (LULC) including water consumption patterns. Unplanned urbanization and increasing human activities are responsible for changes in groundwater regime (Kumar and Pandey 2016). In most of the cases, pumping is more than the amount of annual recharge. Worldwide, various river basins have poor surface water and groundwater quality because of surface water and groundwater interaction problem (Sakai et al. 2018). Thus groundwater quantity and quality analysis are required for a sustainable groundwater management plan. In the present research, future scenarios were generated based on groundwater potential zones with fifteen hydro-geo-meteorological variables. A quality zone map was also generated based on twelve water quality parameters to depict the present scenario.

No research work is available on the generation of future scenarios of groundwater potential zones considering climate and LULC change. Identification of groundwater potential zones with hydrogeological parameters is a very common approach. Nampak et al. (2014) presented spatial prediction of groundwater productivity based on an evidential belief function model. A total 60 wells are utilized for training (42) and validation (18) purposes with higher yield cutoff point at discharge $\geq 1 \text{ m}^3/\text{h}$. Velasco et al. (2014) provided the spatial distribution of hydrogeochemical maps for the city of Badalona. Zaidi et al. (2015) delineated a artificial groundwater recharge zone map using Boolean logic for Northwestern Saudi Arabia. The results were classified on the basis of high priority and low priority zones. It was found that 17.90% area was suitable for recharge without considering LULC features. Rahmati et al. (2016) performed groundwater potential zoning using random forest and maximum entropy models in Mehran Region, Iran. A total 163 wells were used for training (114 wells) and validation (49 wells) purposes. Kumar and Pandey (2016) analyzed groundwater fluctuation trends based on time series regression and the least square method. It was observed that 17%, 13%, 8.07% and 9.61% of northern, south-western, southern and eastern have high to low groundwater recharge potential. Dhanasekarapandian et al. (2016) studied spatiotemporal water quality mapping for drinking and irrigation in the urban reach of the Gridhumal river sub-basin. Maheswaran et al. (2016) studied the effects of stream-aquifer interaction by considering losing and gaining stretches in the Ganga River Basin using Visual MODFLOW. Mahmoud and Kotb (2017) identified the suitable location of groundwater extraction using Vertical Electrical Sounding (VES) in the West Bani Mazar area, El Minia Western Desert, Egypt. Naghibi et al. (2017) performed groundwater well potential zoning by data mining algorithms for the Kashmar Region. Zahedi (2017) used indices for drinking and irrigation water to obtain water quality ranking in agricultural societies with a multi-criteria decision making (MCDM) framework. Amineh et al. (2017) identified suitable areas for aquifer storage using the MCDM technique. Prasad and Rao (2018) analyzed groundwater depletion and balance based on groundwater levels at 41 observation wells during 2013–2015 in the Kandivalasa River. Chen et al. (2018) produced groundwater spring potential zone maps based on the ensemble model and machine learning technique using 14 affecting factors. Multicollinearity analysis technique also used to optimize the affecting factors. Mogaji and San Lim (2018) demarcated the groundwater productivity potential index (GPPI) map using evidential belief function from hydrogeological and geophysical data. Aquifer transmissivity, hydraulic conductivity and resistivity data were utilized for generation of potential map. Das and Pal (2019) identified the groundwater recharge

potential zones based on the Fuzzy-Analytical Hierarchy Process (AHP) in the Goghat II block of West Bengal. High GWPZ (10.13%) covers the north-eastern part of the block because of a low lying flat plain. Achu et al. (2020) demarketed GWPZ using MCDM techniques in the tropical Manimala River Basin (MRB) in Kerala, India. Various geoenvironmental factors (eg. Lithology, geomorphology) were utilized to generate the GWPZ. A total 50% and 20% of the basin area comes under poor, moderate, and good GWPZ. Conjunctive use of water is an integral part of water resources management (Panagopoulos et al. 2012). However, future water availability estimation is a difficult task. Specifically, future groundwater availability scenario generation is important under changing climatic condition. The present research focused on generation of future scenarios of groundwater with regional scale CMIP5 data. Future LULC maps were generated by using the Dyna-CLUE model. MIROC5 model (RCP 4.5) data were utilized for generation of future scenarios of climate change. Raju et al. (2017) presented an intercomparison of global climate models for temperature data. MIROC5 was identified as the most suitable model for the present study area. Future recharge and ET maps were produced through the SWAT (hydrological model). Groundwater table maps for future were also produced using MODFLOW. Finally, future and present parameters were combined for future groundwater potential zone identification in the Dwarakeswar-Gandheswari basin. Sensitivity analysis was performed for groundwater potential and quality mapping.

2 Study Area

Dwarakeswar, an eastern flowing river, originates from Tilboni hill (Fig. 1). Gandheswari is the major tributary (Sahoo et al. 2018). Three hydraulic structures and corresponding command areas are planned within the Dwarakeswar-Gandheswari river basin (Sahoo et al. 2019a; Sahoo et al. 2019b).

3 Material and Methods

3.1 Data Sources

Landsat images were obtained from Earth Explorer (<http://earthexplorer.usgs.gov/>). RCPs data were obtained from the Intergovernmental Panel on Climate Change (IPCC) Fifth Assessment Report (<http://gisweb.ciat.cgiar.org>). Precipitation and temperature data (1979–2014) were obtained (grid: $0.5^\circ \times 0.5^\circ$) from the National Centers for Environmental Prediction (NCEP) Climate Forecast System Reanalysis (CFSR) [<https://globalweather.tamu.edu>]. Groundwater quality and water level data were obtained from the Central Ground Water Board.

3.2 Methodology

3.2.1 Future LULC Change Predictions

Dyna-CLUE simulates land-use types dynamically (Verburg et al. 2002) with five parameters, e.g., land-use demand, location suitability, neighborhood suitability, spatial restriction and conversion parameter. Sahoo et al. (2018) studied the LULC change in detail.

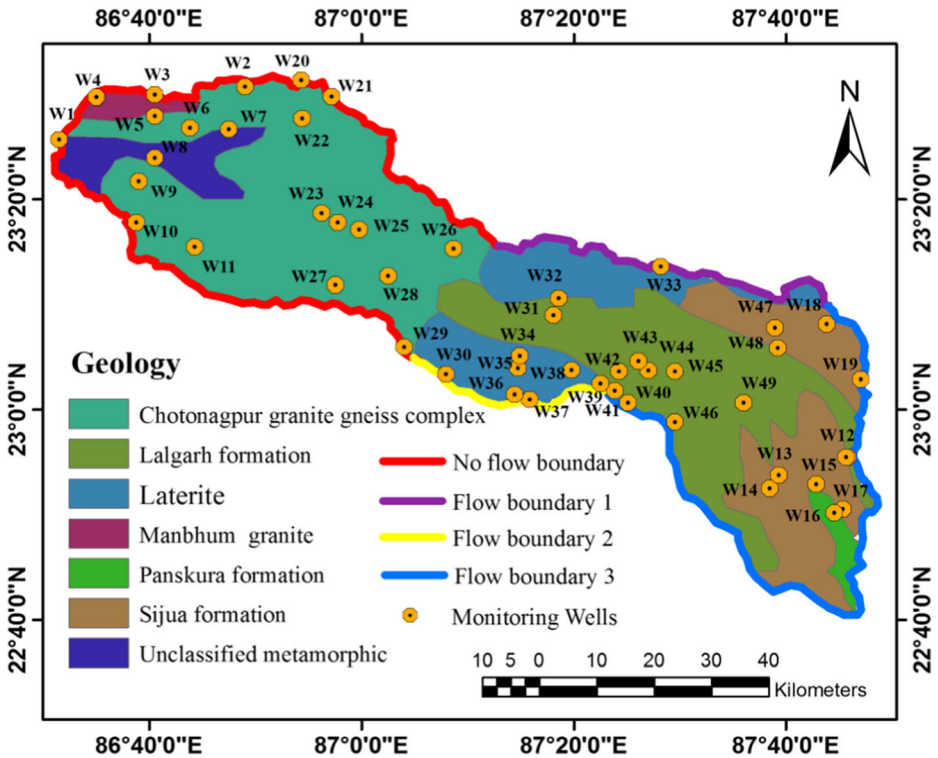


Fig. 1 Location map of the study with boundary condition

3.2.2 Future Climate Change Predictions

MIROC5 model data was used for groundwater potential scenario generation under changing climatic conditions. The bias-corrected rainfall and temperature (RCP 4.5) data were obtained using the Linear scaling (LS) and distribution mapping (DM) methods (Fang et al. 2015). The rainfall and temperature spatial distribution maps were generated using Inverse distance weighted (IDW) method. Future rainfall and temperature data were utilized for generation of future GWPZ map.

3.2.3 Future Groundwater Recharge Predictions

The recharge is a major component for the assessment of aquifer health. Recharge rate depends on the hydraulic properties. Sahoo et al. (2019a) estimated the recharge.

3.2.4 Future Population Predictions

Population plays a critical role in groundwater planning as it controls food, water and energy nexus. Population projection is required for future demand management. Exponential growth rate based population can be calculated as (De Andreis and Ricci 2005)

$$N(t) = N_0 e^{rt} \tag{1}$$

Where, t = time, r = relative growth rate, N_0 = initial population, and $N(t)$ = population after a time t has passed.

3.2.5 Future Groundwater Table Predictions

The transient Modular Three-Dimensional Finite-Difference Groundwater Flow (MODFLOW) was utilized for regional-scale hydraulic head simulation model (Harbaugh 2005; Guzman et al., 2015 and Wei et al. 2018). MODFLOW requires elevation, groundwater level, hydraulic conductivity, specific yield, recharge rate, streamflow, pumping considering water demand.

3.2.6 Groundwater Potential Index (GWPI)

Potential zones of groundwater can be estimated as (Dhar et al. 2015)

$$GWPI_{i,j} = \sum_{k=1}^{|F|} W_k \left[\sum_{l=1}^{|S_k|} w_l^k \chi_{C_l^k} (p_{i,j}|_k) \right] \tag{2}$$

where indices i and j represents row and column for a pixel; $|F|$ denotes the total number of features in set F ; $|S_k|$ denotes the total number of sub-features for k^{th} feature in set S_k ; W_k normalized weight of k^{th} feature; w_l^k normalized weight of l^{th} sub-feature for k^{th} feature; $p_{i,j}|_k$ denotes pixel value for a sub-feature for k^{th} feature; C_l^k denotes the sub-feature class, $\chi_{C_l^k}$ denotes the class indicator function.

$$\chi_{C_l^k} (p_{i,j}|_k) = \begin{cases} 1 & \text{if } p_{i,j}|_k \in C_l^k \\ 0 & \text{if } p_{i,j}|_k \notin C_l^k \end{cases} \tag{3}$$

3.2.7 Groundwater Quality Index (GWQI)

Groundwater quality index (GWQI) can be estimated as (Dhar et al. 2015)

$$GWQI_{i,j} = \Lambda_{i,j} \sum_{k=1}^{|F|} W_k \left[\sum_{l=1}^{|S_k|} w_l^k \chi_{C_l^k} (p_{i,j}|_k) \right] \tag{4}$$

where, $\Lambda_{i,j}$ is a water quality correction factor for the above standard limit (ASL) values. $\Lambda_{i,j}$ is defined as

$$\Lambda_{i,j} = \prod_{k=1}^{|F|} \left[\sum_{l=1}^{|S_k|} \xi_k (C_l^k) \chi_{C_l^k} (p_{i,j}|_k) \right] \tag{5}$$

with $\xi_k (C_l^k)$ as the water quality indicator function.

$$\xi_k (C_l^k) = \begin{cases} 1 & \text{if } C_l^k \text{ represents BSL interval} \\ 0 & \text{if } C_l^k \text{ represents ASL interval} \end{cases} \tag{6}$$

Water quality indicator function takes binary value (=1) for below standard level (BSL) interval. W_k and w_l^k can be estimated by using Analytic Hierarchy Process (Saaty 1980;

Alonso and Lamata 2006). Details of the calculation procedures are available in Bathrellos et al. (2012); Dhar et al. (2015); Bathrellos et al. (2017).

4 Results

Groundwater quantity and quality analysis were performed using AHP framework. AHP was used for effectiveness evaluation of regional groundwater scenarios.

4.1 Delineation of Future Groundwater Potential Zones

Fifteen parameters [aspect (AS), elevation (EL), slope (SL), soil texture (ST), geology (GG), *future* LULC (FL), drainage density (DD), *future* rainfall (FR), *future* maximum temperature (FMAT), *future* minimum temperature (FMIT), soil moisture (SM), *future* evapotranspiration (ET), *future* groundwater level (GL), *future* recharge (RR) and normalized difference vegetation index (NDVI)] were considered for delineation of future groundwater potential zones (GWPZ).

Aspect, elevation, and slope maps were prepared from the SRTM DEM using the GIS platform. Aspect indicates the slope direction. Flat areas correspond to moderate groundwater prospect zone. Lower slope (approximately <52 m) is suitable for groundwater recharge.

Soil and geology are more significant for groundwater prospect/recharge mapping. The maximum area covers by the fine and fine loamy soil. The groundwater movement depends on geological materials through an aquifer.

Future LULC maps were prepared by using the Dyna-CLUE model based on various hydro-geological parameters. The Dyna-CLUE model generated future LULC maps for the years 2030, 2050, 2080 (Sahoo et al. 2018) were classified into seven categories: barren land, built-up land, cropland, forest land, fallow land, shrubland, water bodies. Cropland covers the maximum area. Built-up land covers the downstream region of the river basin. Bankura is the main town within the study area. The drainage density map was generated from SRTM DEM data. The high and low permeable rock formation depends on coarse and fine drainage textures. The rainfall and temperature distribution is very importance for groundwater potential zoning. Rainfall and temperature (both maximum and minimum) maps for future were prepared from RCP 4.5 regional climate model data.

Soil moisture data was utilized for identification of groundwater potential scenario. Soil moisture data were calculated by the NOAH model ($0.25^\circ \times 0.25^\circ$, monthly data) with the Global Data Assimilation System (GLDAS). The FAO Penman-Monteith (FAO-PM) method was utilized for the satellite images to calculate ET values. Higher ET value show correspondence with the higher elevated area (Susunia hill, Tilabani hill). The operational land imager (OLI) multispectral images were utilized for ET mapping. The SWAT model was used for the generation of future ET mapping purposes.

4.2 Modular Three-Dimensional Finite-Difference Groundwater Flow

The recharge, natural discharge and abstraction are crucial parameters for fluctuation of groundwater level. The present groundwater level map (below ground level, bgl) was classified into five categories: (i) <2.82 m bgl (34.17%), (ii) 2.82–5.03 m bgl (41.57%), (iii) 5.03–8.25 m bgl (9.19%), (iv) 8.25–11.63 m bgl (12.83%), and, (v) >11.63 m bgl (2.24%). The future

groundwater level maps were generated from MODFLOW. A total 49 observation wells (2002–2017) were selected for groundwater level modeling. The past and future recharge and ET (considers to pumping) were estimated by hydrological modeling. The future population growth data was generated based on past and present census data (Fig. 2). Five blocks (Khanakul 1, Onda, Arambagh, Garbeta and Para) showed the maximum population increase. The horizontal and vertical hydraulic conductivity and specific yield data were considered at block level. The conductivity values based on local geology were adjusted through trial and error approach (Freeze and Cherry 1979). The recharge and pumping data were also considered at the sub-watershed level. The flow boundary was demarcated from geological conditions in the river basin. A single-layered aquifer of 30 m thickness was considered. The observed and hydrological model-based estimated streamflow values were considered as specific flow in the river. Finally, all data were integrated in MODFLOW for generation of past and future groundwater level maps. The past simulated groundwater head value varies between 0 to 384 m (with respect to mean sea level) for 2010. The generated future groundwater head values vary between 0 and 400 m for 2030 to 2080 time periods. Low groundwater head (0–50 m) was observed in the lower part of the river basin. Moderate and high groundwater head regions were corresponds to the middle and upper part of the river basin. Visible changes in groundwater table was observed between the years 2010 and 2030. The calibration (2002–2011) and validation (2012–2017) were performed in transient mode (Figs. 3 and 4). Box plot maps are produced through 2 m observation transient head interval from MODFLOW. The difference between simulated and observed groundwater heads is maximum for a few wells corresponding

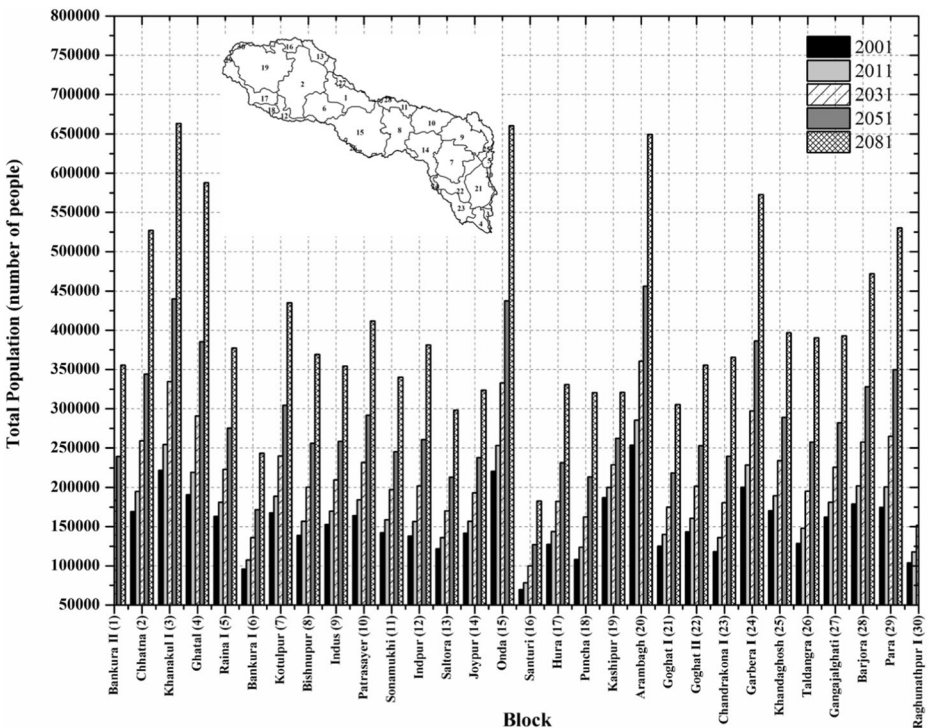
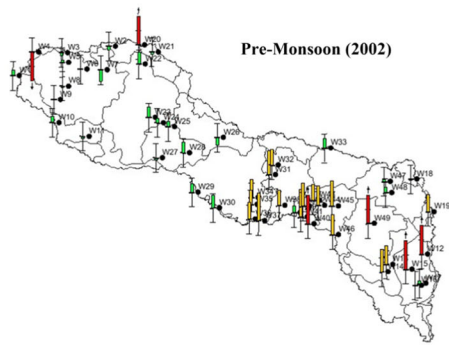
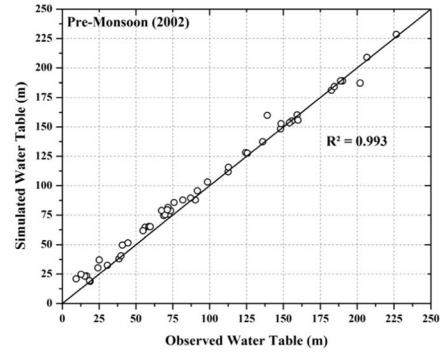


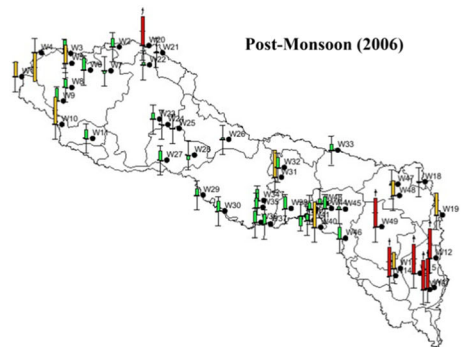
Fig. 2 Past and Future trend of population for 2001, 2011, 2031, 2051 and 2081



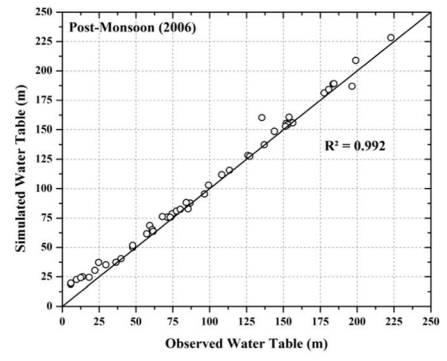
(a)



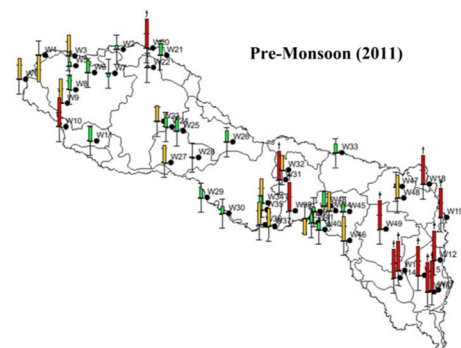
(b)



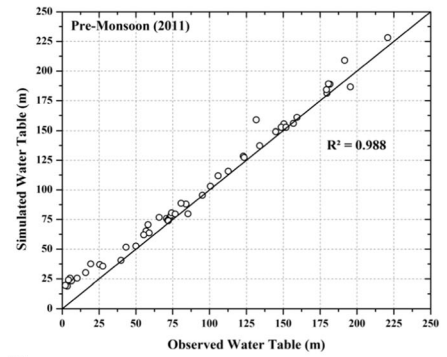
(c)



(d)



(e)



(f)

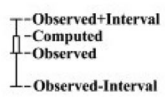
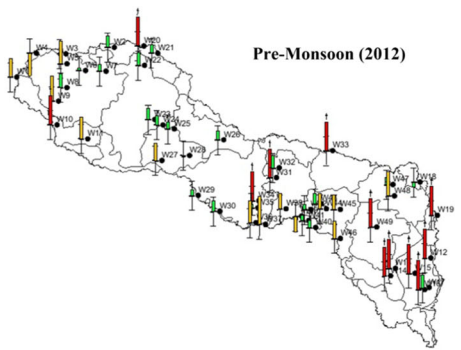
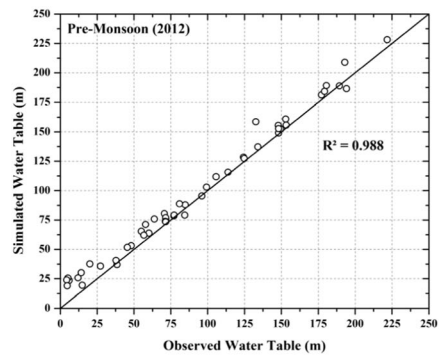


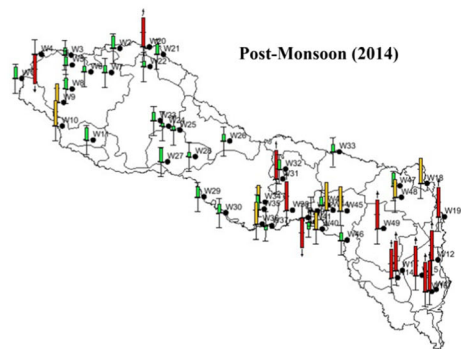
Fig. 3 Calibration of the MODFLOW Model



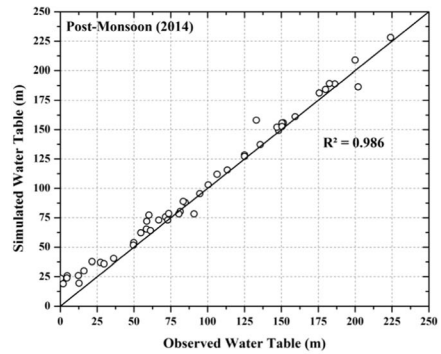
(a)



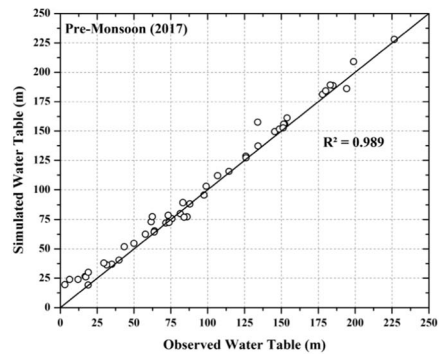
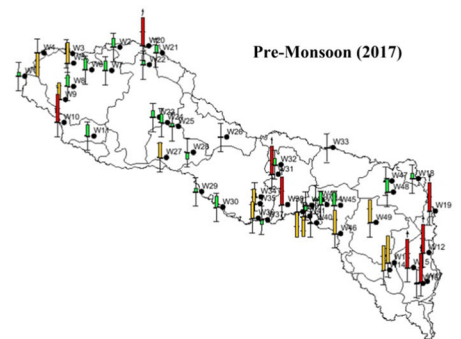
(b)



(c)



(d)



—|— Observed+Interval
 —|— Computed
 —|— Observed
 —|— Observed-Interval

Fig. 4 Validation of the MODFLOW Model

to regions with maximum built-up areas. This difference is due to local changes in observed groundwater levels which cannot be captured through a regional groundwater model. All results

are satisfactory under regional scale conditions. Future groundwater recharge maps (2010–2080) were generated using the SWAT model.

4.3 Groundwater Potential Zone Mapping with Validation

Future groundwater potential zone mapping was performed through the three model generated seven futuristic parameters. Detailed normalized weights calculation process is available in Sahoo et al. (2019a, 2019b). Four GWPZ scenarios were generated (Fig. 5) for the year of 2010, 2030, 2050 and 2080 and output maps were classified into three classes (poor potential, moderate potential and good potential). Upper portion of the river basin was identified as poor GWPZ for the years 2010 and 2030. However, middle portion of the river basin was identified as poor GWPZ for the year 2080. Finally, output maps were validated by using field soil moisture data (dry, dry+, wet and wet+) and groundwater level. It was found that wet and wet+ soil moisture points were within the good GWPZ areas.

4.4 Groundwater Quality Zone Mapping

The groundwater pollution scenario gets affected by various hydro-geological parameters (e.g. LULC, slope, soil). In the present work, twelve parameters (pH, Cl^- , Mg^{2+} , F^- , Na^+ , EC, TH, HCO_3^- , K^+ , Ca^{2+} , SO_4^{2-} and PO_4^{2-}) were used for groundwater quality index (GWQI) calculation. The measurement of pH is very important for water treatment. pH represents the alkalinity and acidity of groundwater. High pH values are obtained for the W1, W3, W4, W5, W7, W10, W11, W41, W43, W68, W70, and W73. Electrical Conductivity (EC) is a

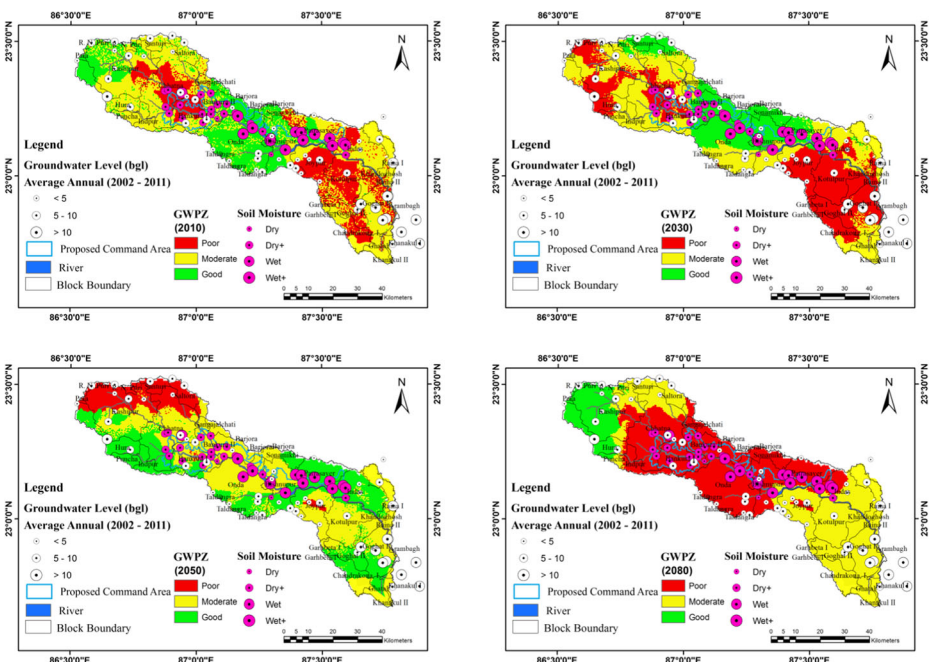


Fig. 5 Future scenarios of groundwater potential zone mapping

significant factor for irrigation purposes. Increased EC means the presence of more ions in the water. W66 and W57 have the highest EC in the upstream region. Minimum and maximum values of TH are 42.31 mg/L and 1603.25 mg/L in the river basin. Higher TH values are visible for the W1, W2, W3, W4, W5, W9, W10, W57 and W66.

Calcium and magnesium have serious importance to human health. Groundwater is the main source of these ions. Ca block absorption of heavy metals in the human body. The result shows W57 and W66 are above the permissible limits in the upstream region. A highly urbanized part (downstream part of the river basin) shows Mg values above permissible limit. The concentration of Na ranges between <200 mg/L to 566 mg/L in groundwater. W57 and W66 have a high sodium concentration in the upper portion of the river basin. Increased sodium levels in groundwater may indicate pollution from the point or non-point sources. Potassium and sodium are very important chemical parameters for groundwater. These chemicals are found in rock and soils. Potassium can also be found in fertilizers. W56 has a high K⁺ concentration. Non-calcareous aquifers are sources of bicarbonate. Groundwater with high HCO₃ indicates a high pH level. The results show that W57 and W66 have high concentrations. Chloride comes from both natural and anthropogenic sources. Chloride is available in inorganic fertilizer, landfill leachates, irrigation drainage and seawater intrusion in coastal areas. W54 and W57 show high chloride concentration.

Fluoride, sulfate, and phosphate are prime factors in groundwater quality. Low fluoride concentration is advantageous for dental health. High fluoride (>1.5 mg/L) concentration invites fluorosis. W53 and W67 (located in the upstream portion of the river basin) have F⁻ concentration above the permissible limit. Low fluoride concentration covers a maximum area within the river basin. The spatial distribution results show that <200 mg/L values are scattered over the whole study area. Phosphate is a prime factor for organisms and plants. It is not a risk to groundwater. However, it is a key factor for seasonal cropping patterns. W16, W17, W20, W50, and W66 have high phosphate concentration.

4.5 Groundwater Quality Zone Mapping Using GIS Technique

Groundwater quality analysis was performed by twelve physicochemical parameters. Detailed weight calculation procedures are available in Dhar et al. (2015) and Sahoo et al. (2019a, 2019b). The resulting maps (Fig. 6) were classified into four classes (above the permissible limit, poor, moderate, and good). It was observed that seventeen wells within the above permissible limit region. The maximum above permissible region covers the lower part or urbanized part of the river basin.

Parameter sensitivity analysis showed that recharge, ET, rainfall, soil and geology were more significant parameters for GWPZ (Table 1). However, pH, EC, Na, K, HCO₃ and PO₄ were relatively significant for GWQZ (Table 2). The overall methodology (GWPZ & GWQZ) is schematically presented in Fig. 7.

5 Discussion

The multi-criteria decision making (MCDA) technique was used for delineation of groundwater potential and quality zones by using remote sensing and GIS environment. Only a few researchers have used the MCDA technique for groundwater quantity and quality analysis (Dhar et al. 2015; Kumar and Pandey 2016; Jasrotia et al., 2018). However, no study has ever

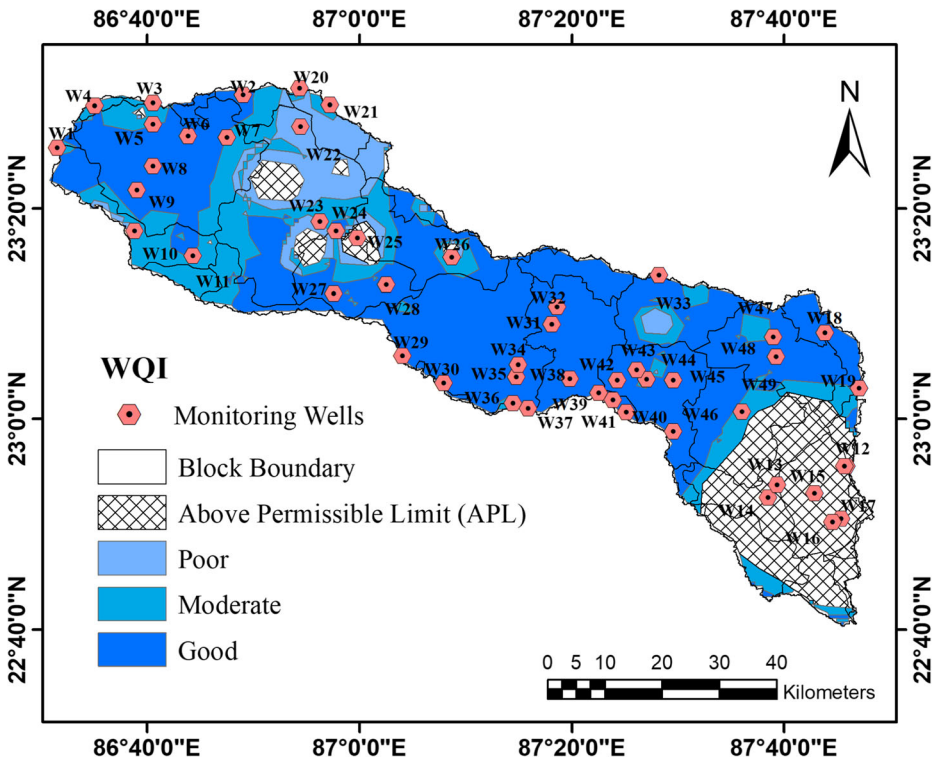


Fig. 6 Water quality zone maps using GIS platform

attempted the generation of future groundwater potential zone maps under changing climatic conditions. Seven future parameters (LULC, rainfall, maximum and minimum temperature,

Table 1 Area under different classes change with exclusion of each groundwater potential parameter

i		% Change		
		Poor	Moderate	Good
1	Aspect	-13.98	+7.95	+6.03
2	Elevation	-12.33	+7.26	+5.06
3	Slope	-13.59	+8.28	+5.31
4	Soil	-13.97	+6.75	+7.22
5	Geology	-11.92	+4.40	+7.52
6	LULC	-7.92	+1.72	+6.20
7	Drainage Density	-14.04	+8.62	+5.46
8	Rainfall	-13.28	+4.72	+8.56
9	Maximum Temperature	-13.34	+5.48	+7.86
10	Minimum Temperature	-11.52	+5.10	+6.41
11	Soil Moisture	-13.69	+6.55	+7.14
12	ET	-14.69	+8.20	+6.49
13	Groundwater Level	-15.93	+11.26	+4.67
14	Recharge	-18.95	+7.11	+11.83
15	NDVI	-13.35	+7.70	+5.64
S_F	All parameters	24.4	49.61	25.99

Bold values indicate significant results

Table 2 Area under different classes change with exclusion of each groundwater quality parameter

<i>i</i>		Above Permissible Limit	Poor	% Change Moderate	Good
1	pH	–	+1.0	+1.93	–21.31
2	EC	–	+0.5	–3.68	–15.21
3	TH	+0.05	–0.25	+2.0	–1.79
4	Ca	+0.05	–0.9	–0.45	+1.31
5	Mg	+0.05	–0.28	+1.61	–1.39
6	Na	–	–1.28	–2.47	–14.64
7	K	–	–0.32	–3.87	–14.21
8	HCO₃	–	–1.21	–3.37	–13.81
9	Cl	+0.05	+0.64	+3.31	–4.0
10	F	+0.05	+0.98	–4.51	+3.47
11	SO₄	+0.05	–0.76	–1.25	+1.97
12	PO₄	–	–0.71	–2.92	–14.77
<i>S_F</i>	All parameters	18.39	7.99	18.84	54.78

Bold values indicate significant results

recharge, groundwater table and ET) were utilized for the groundwater potential mapping. The SWAT hydrological model was utilized for groundwater recharge and ET calculation purposes (Dhar et al. 2015; Fukunaga et al. 2015; Mechal et al. 2015). Regional climate model data (RCP 4.5) were utilized for future rainfall and maximum and minimum temperature estimation purpose (Kim et al. 2015; Kwon and Lee 2015). In the present study, the AHP method is used for the generation of GWPZ and GWQZ by various hydrogeological and physicochemical parameters (Dhar et al. 2015; Kumar and Pandey 2016; Sahoo et al. 2019a, 2019b). However, the AHP is a state forward structured technique for analyzing complex decisions and quantifying the weights of decision criteria (Saaty 1980; Alonso and Lamata 2006). Finally, future groundwater potential maps were successfully delineated for the Dwarakeswar-Gandheswari river basin.

6 Conclusions

In the present research, groundwater quantity and quality analysis were performed for a small tropical river basin for the generation of groundwater scenarios. The research focuses on the

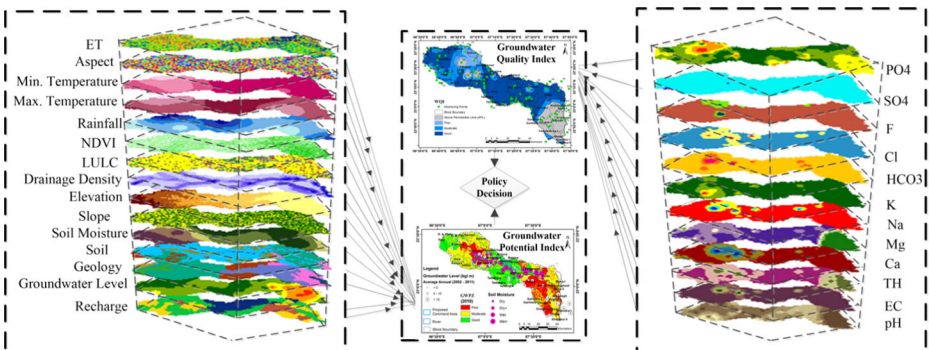


Fig. 7 Graphical representation of overall methodology in this research

generation of future scenarios (2030–2050–2080) of groundwater potential zones (GWPZs) using seven futuristic parameters (LULC, maximum and minimum temperature, rainfall, recharge, groundwater level, and ET) from four different simulation models (Dyna-Clue, RCM, SWAT and MODFLOW). SWAT and MODFLOW were used for groundwater recharge, ET, and groundwater level estimation purposes. However, fifteen parameters for GWPZ and twelve parameters for GWQZ were utilized for spatial distribution mapping using the geospatial platform. Field-based soil moisture (37 points location) and groundwater monitoring point (49 wells) data were used for validation purposes. Sensitivity analysis revealed that recharge, ET, rainfall, soil, and geology were highly sensitive features for groundwater potential. The water quality results show that the downstream portion (Khandoghosh, Raina I, Goghat, Chandrakona, Ghatal, and Khanakul blocks) of the river basin has the above permissible limit areas. Groundwater quality results also show Bankura town, Chhatna and inside areas in the river basin are under above permissible limit zone. The middle portion of the river shows good quality of groundwater. pH, EC, Na, K, HCO₃, and PO₄ were more sensitive parameters for GWQZ. The lower part of the river basin shows poor groundwater potential (13.02% for 2050) and poor groundwater quality zone due to the presence of built-up areas. Groundwater potential and quality maps will be useful for development of sustainable water management plan.

Compliance with Ethical Standards

Conflict of Interest No conflict of interest.

References

- Achu AL, Thomas J, Reghunath R (2020) Multi-criteria decision analysis for delineation of groundwater potential zones in a tropical river basin using remote sensing, GIS and analytical hierarchy process (AHP). *Groundw Sustain Dev*, 100365
- Alonso J, Lamata T (2006) Consistency in the analytic hierarchy process: a new approach. *Int J Uncertainty Fuzziness Knowledge Based Syst* 14(4):445–459
- Aminch ZBA, Hashemian SJAD, Magholi A (2017) Integrating Spatial Multi Criteria Decision Making (SMCDM) with Geographic Information Systems (GIS) for delineation of the most suitable areas for aquifer storage and recovery (ASR). *J of hydro* 551:577–595.
- Bathrellos GD, Gaki-Papanastassiou K, Skilodimou HD, Papanastassiou D, Chousianitis KG (2012) Potential suitability for urban planning and industry development using natural hazard maps and geological–geomorphological parameters. *Environ Earth Sci* 66(2):537–548
- Bathrellos GD, Skilodimou HD, Chousianitis K, Youssef AM, Pradhan B (2017) Suitability estimation for urban development using multi-hazard assessment map. *Sci Total Environ* 575:119–134
- Chen W, Li H, Hou E, Wang S, Wang G, Panahi M, Xiao L (2018) GIS-based groundwater potential analysis using novel ensemble weights-of-evidence with logistic regression and functional tree models. *Sci Total Environ* 634:853–867
- Das B, Pal SC (2019) Combination of GIS and fuzzy-AHP for delineating groundwater recharge potential zones in the critical Goghat-II block of West Bengal, India. *HydroResearch* 2:21–30
- De Andreis S, Ricci PE (2005) Modelling population growth via loguerre-type exponentials. *Math Comput Model* 42(13):1421–1428
- Dhanasekarapandian M, Chandran S, Devi DS, Kumar V (2016) Spatial and temporal variation of groundwater quality and its suitability for irrigation and drinking purpose using GIS and WQI in an urban fringe. *J Afr Earth Sci* 124:270–288
- Dhar A, Sahoo S, Sahoo M (2015) Identification of groundwater potential zones considering water quality aspect. *Environ Earth Sci* 74(7):5663–5675

- Fang GH, Yang J, Chen YN, Zammit C (2015) Comparing bias correction methods in downscaling meteorological variables for a hydrologic impact study in an arid area in China. *Hydrol Earth Syst Sci* 19(6):2547–2559
- Freeze RA, Cherry JA (1979) *Groundwater*, 604 pp.
- Fukunaga DC, Cecilio RA, Zanetti SS, Oliveira LT, Caiado MAC (2015) Application of the SWAT hydrologic model to a tropical watershed at Brazil. *Catena* 125:206–213
- Guzman JA, Moriasi DN, Gowda PH, Steiner JL, Starks PJ, Arnold JG, Srinivasan R (2015) A model integration framework for linking SWAT and MODFLOW. *Environ Modelling & Software*, 73:103–116.
- Harbaugh A W (2005) MODFLOW-2005, the US geological survey modular ground-water model: the ground-water flow process (p. 253). Reston, VA: US Department of the Interior, US Geol Surv
- Jasrotia AS, Ajay KT, Upasna A, Baghwan DB (2018) Geoinformatics based groundwater quality assessment for domestic and irrigation uses of the Western Doon valley, Uttarakhand, India. *Groundw for Sustain Dev* 6: 200–212
- Kim KH, Cho J, Lee YH, Lee WS (2015) Predicting potential epidemics of rice leaf blast and sheath blight in South Korea under the RCP 4.5 and RCP 8.5 climate change scenarios using a rice disease epidemiology model, EPIRICE. *Agric For Meteorol* 203:191–207
- Kumar A, Pandey AC (2016) Geoinformatics based groundwater potential assessment in hard rock terrain of Ranchi urban environment, Jharkhand state (India) using MCDM–AHP techniques. *Groundw Sustain Dev* 2:27–41
- Kwon TS, Lee CM (2015) Prediction of abundance of ants according to climate change scenarios RCP 4.5 and 8.5 in South Korea. *J Asia Pac Biodiv* 8(1):49–65
- Maheswaran R, Khosa R, Gosain AK, LahariS SSK, Chahar BR, Dhanya CT (2016) Regional scale groundwater modelling study for Ganga River basin. *J Hydrol* 541:727–741
- Mahmoud HH, Kotb ADM (2017) Impact of the geological structures on the groundwater potential using geophysical techniques in west BaniMazar area, El Minia–Western Desert, Egypt. *J Afr Earth Sci* 130:161–173
- Mechal A, Wagner T, Birk S (2015) Recharge variability and sensitivity to climate: the example of GidaboRiver Basin, Main Ethiopian rift. *J Hydrol Reg Stud* 4:644–660
- Mogaji KA, San Lim H (2018) Application of Dempster-Shafer theory of evidence model to geoelectric and hydraulic parameters for groundwater potential zonation. *NRIAG J Astron Geophys*,
- Naghbi SA, Moghaddam DD, Kalantar B, Pradhan B, Kisi O (2017) A comparative assessment of GIS-based data mining models and a novel ensemble model in groundwater well potential mapping. *J Hydrol* 548:471–483
- Nampak H, Pradhan B, Manap MA (2014) Application of GIS based data driven evidential belief function model to predict groundwater potential zonation. *J Hydrol* 513:283–300
- Panagopoulos GP, Bathrellos GD, Skilodimou HD, Martsouka FA (2012) Mapping urban water demands using multi-criteria analysis and GIS. *Water Resour Manag* 26(5):1347–1363
- Prasad YS, Rao BV (2018) Groundwater depletion and groundwater balance studies of KandivalasaRiverSubBasin, Vizianagaram District, Andhra Pradesh, India. *Groundw Sustain Dev* 6:71–78
- Rahmati O, Pourghasemi HR, Melesse AM (2016) Application of GIS-based data driven random forest and maximum entropy models for groundwater potential mapping: a case study at Mehran region, Iran. *Catena* 137:360–372
- Raju KS, Sonali P, Kumar DN (2017) Ranking of CMIP5-based global climate models for India using compromise programming. *Theor Appl Climatol* 128(3–4):563–574
- Saaty TL (1980) *The analytic hierarchy process: planning, priority setting, resource allocation*. McGraw-Hill, New York
- Sahoo S, Sil I, Dhar A, Debsarkar A (2018) Das P Kar a (2018) future scenarios of land-use suitability modeling for agricultural sustainability in a river basin. *J Clean Prod* 205:313–328
- Sahoo S, Dey S, Dhar A, Debsarkar A, Pradhan B (2019a) On projected hydrological scenarios under the influence of bias-corrected climatic variables and LULC. *Ecol Indic* 106:105440
- Sahoo S, Dhar A, Debsarkar A, Kar A (2019b) Future scenarios of environmental vulnerability mapping using grey analytic hierarchy process. *Nat Resour Res* 28(4):1461–1483
- Sakai N, Mohamad ZF, Nasaruddin A, Kadir SNA, Salleh MSAM, Sulaiman AH (2018) Eco-heart index as a tool for community-based water quality monitoring and assessment. *Ecol Indic* 91:38–46
- Velasco V, Tubau I, Vázquez-Suñè E, Gogu R, Gaitanaru D, Alcaraz M, Sanchez-Vila X (2014) GIS-based hydrogeochemical analysis tools (QUIMET). *Comput Geosci* 70:164–180
- Verburg PH, Soepboer W, Veldkamp A, Limpiada R, Espaldon V, Mastura SS (2002) Modeling the spatial dynamics of regional land use: the CLUE-S model. *Environ Manag* 30(3):391–405

- Wei X, Bailey RT, Records RM, Wible TC, Arabi M (2018) Comprehensive simulation of nitrate transport in coupled surface-subsurface hydrologic systems using the linked SWAT-MODFLOW-RT3D model. *Environ Model Softw*
- Zahedi S (2017) Modification of expected conflicts between drinking water quality index and irrigation water quality index in water quality ranking of shared extraction wells using multi criteria decision making techniques. *Ecol Indic* 83:368–379
- Zaidi FK, Nazzal Y, Ahmed I, Naeem M, Jafri MK (2015) Identification of potential artificial groundwater recharge zones in northwestern Saudi Arabia using GIS and Boolean logic. *J Afr Earth Sci* 111:156–169

Publisher's Note Springer Nature remains neutral with regard to jurisdictional claims in published maps and institutional affiliations.

Affiliations

Satiprasad Sahoo¹ · Anirban Dhar² · Anupam Debsarkar³ · Amlanjyoti Kar⁴

¹ School of Ecology & Environment Studies, Nalanda University, Bihar, Rajgir 803116, India

² Department of Civil Engineering, Indian Institute of Technology Kharagpur, Kharagpur, India

³ Department of Civil Engineering, Jadavpur University, Kolkata, India

⁴ Superintending Hydrogeologist, Central Ground Water Board, Kolkata, India